Sealability Recovery of Fractured Rocks by Post-failure Consolidation

Y. Fujii[a]*, S. Kumakura[b] and K. Kaneko[c]

[a]*Hokkaido University, Sapporo, Japan*
[b]*DOCON Co. Ltd., Sapporo, Japan*
[c]*H-RISE, Horonobe, Japan*
*fujii6299@frontier.hokudai.ac.jp (*corresponding author's E-mail)*

Abstract

Post-failure consolidation was carried out on Kimachi sandstone, Toyotomi siliceous mudstone and Inada granite to clarify whether the increased hydraulic conductivity due to failure decreased by post-failure consolidation or not. The hydraulic conductivity of post-failure consolidated rocks were 0.3-0.6 times that before post-failure consolidation and 0.9-1.5 times that before failure for Kimachi sandstone and the ratios were 0.4 times and 0.6 times for Toyotomi siliceous mudstone. On the other hand, the ratio was 0.2 times and 16 times for Inada granite. Namely, the phenomenon in which the increased hydraulic conductivity decreases by post-failure consolidation was obviously confirmed for the clastic rocks and was confirmed at some degree for the crystalline rock. The dominating mechanisms of decrease in hydraulic conductivity due to the post-failure consolidations were considered to be closure of rupture plane by crushing of mineral particles and irrecoverable closure of microcracks and elliptic pores in intact rock matrix due to plastic deformation for Kimachi sandstone, time-dependent closure of rupture plane due to visco-plastic deformation and visco-plastic pore collapse in intact rock matrix for Toyotomi siliceous mudstone, and a little visco-plastic deformation and a few pressure solution at the rupture plane for Inada granite. The different mechanisms were mainly induced by the differences in strength and deformation characteristics of mineral particles and rock matrixes.

Keywords: Sealability Recovery, Fractured Rocks, Triaxial Compression, Post-failure Consolidation

1. Introduction

EDZ (Excavation Damaged Zone) and EdZ (Excavation disturbed Zone) will appear around such underground openings as underground LPG storage tanks, geological storage sites for nuclear wastes etc. The former is the zone with irrecoverable damages by stress concentration etc. due to excavation and the latter is the zone with elastic disturbances (Tsang et al., 2005). Permeability may increase within EDZ and the increase means deterioration of sealability of the opening. The deterioration is not welcome since it may induce extra costs and time for construction. From this point of view, mechanical and hydrological characteristics of rocks in EDZs were investigated and summarized for crystalline rocks, rock salts, indulated and plastic clays (Tsang et al., 2005). A self healing behavior which is effective to keep sealability was observed for rock salts and clays (Buehler et al., 2003).

There is no descriptions on clastic rocks other than clays in Tsang et al. (2005). Clastic rocks however are also widely distributed over the world including Japan and there is possibility that underground repositories are constructed in clastic rock masses. Not presented as scientific papers but such phenomena as hardening of fractured rocks by reactions from steel arches and that of roof strata without any backfilling at slicing mining activities have been observed in coal mines. They can be considered as a kind of self healing phenomena.

Fujii et al. (2011) observed roadways which were excavated in Paleogene sandstone, shale, sandy shale, siliceous rock and clay as deep as 300 m, and abandoned as early as 50 years ago. Most sections of the roadways had been completely closed by such plastic deformation as roof sag and floor heave except for a few sections where slurry backfilling had not reached. According to their in-situ tests, Rayleigh wave velocity and permeability of the closed roadway were approx. a half and 40 times those of intact rock mass. In their laboratory test, post-failure permeability of sandstone which was sampled at the site decreased to a lower value than that of intact rock with time and further decreased by post-failure consolidation. The repeatability or influences of various conditions were unknown since the test was carried out only once. Xue (1992) triaxially compressed Shirahama sandstone under 7 MPa confining pressure and found that post-failure permeability under 7 MPa hydrostatic pressure

was more than twice that of the intact specimen but the permeability became less than that for the intact specimen after the hydrostatic pressure was raised to more than 12 MPa. Ohishi et al. (2014) compressed cylindrical specimens of siliceous mudstone, Tage tuff, Kawatsu tuff, Kimachi sandstone and Sanjome andesite in a rigid steel ring up to 25% axial strain and measured permeability. All kinds of rock except for the andesite showed decrease in permeability during post-failure consolidation.

From the above studies, it is likely that the permeability of fractured clastic rocks decreases by post-failure consolidation and the decrease amount may larger than that for crystalline rocks. The objective of this research is to experimentally investigate the validity of the above statement under controlled conditions.

It seems rather difficult to precisely control experimental conditions in the rigid ring method by Ohishi et al. (2014) although there are several similarities to in-situ sealability recovery in their experiments. The triaxial compression method by Fujii et al. (2011) was therefore modified and used to carry out post-failure consolidation mainly for Kimachi sandstone as a medium-hard clastic rock. Permeability was occasionally measured before axial compression, around peak stress, under residual strength state, during and after the post-failure consolidation. Toyotomi siliceous mudstone as a soft and weak clastic rock and Inada granite as a hard crystalline rock were also used for the experiment for comparison.

2. Experiments

2.1 Rock specimens

The diameter and length of the specimens were 50 mm and 100 mm respectively. Kimachi sandstone and Inada granite were vacuum-deaired for three days, saturated by distilled water, vacuum-deaired for three days again and stored in distilled water for 30 days and used for the experiments. Toyotomi siliceous mudstone specimens were stored in distilled water for more than one year and used for the experiments.

A pair of endpieces with an axial hole for pore water was attached to each specimen with stainless meshes between the specimen and the endpieces to ensure a uniform pore water flow at the specimen ends. The gap at the specimen side between the endpieces and the specimen was sealed by a plastic and then a self-adhesive tape. Kimachi sandstone and Inada granite were jacketed by a Teflon heat shrinkable tube whereas Toyotomi siliceous mudstone was jacketed by a soft and 1.5 mm thick silicon heat shrinkable tube since the Teflon heat shrinkable tube was rather stiff and might affect the mechanical behavior of the soft rock. A silicon sealant was pasted on the specimen surface before the tube was shrunk to prevent water flow along the boundary between the specimen and the tube. A pair of clamp-type metallic bands was used to seal the specimen from the confining pressure oil.

2.2 Experimental apparatus

Loading was carried out by an MTS815 system (max. load: 4600 kN, max. confining pressure: 80 MPa). Pore pressure was supplied by a syringe pump with max. pressure of 80 MPa. The pore pressure line was connected to the both endpieces via accumulators for the permeability measurement using the simplified transient pulse method. Axial strain was calculated by dividing the displacement from the axial LVDT by the specimen length. Circumferential strain was calculated by dividing the circumferential displacement from a chain type-extensometer by the specimen circumference. Axial and circumferential displacements, axial load, confining and differential pore pressures and water temperature were recorded throughout the experiments.

2.3 Experimental procedure

The loading paths for Cases 1 to 4 (Fig. 1 and Table 1) were used and permeability was ocasionally measured (Fig. 1). The procedure for Case 2 is explained below as an example.

(1) Confining pressure of 1 MPa was applied keeping differential axial stress at 0.5 MPa to know the contact point for precise axial strain calculation.
(2) Prescribed confining and pore pressures in Table 1 were applied and they were kept for 24 hours (consolidation 1).
(3) Axial displacement was applied at a constant circumferential strain rate of -1.9×10^{-6} s^{-1} until residual strength was confirmed or circumferential displacement reached 4 mm (compression 1). The both states in which axial loading was stopped are called "residual strength state" in this paper.
(4) Consolidation 2 was carried out at hydrostatic pressure shown in Table 1. Hydrostatic pressure was basically set at the same value as the residual strength. It however was set at 50% residual

strength for Cases 2-3 and 2-7. The value was set at 30 MPa assuming overburden pressure at 1100 m deep for Inada granite to ensure laboratory safety since the residual strength was too large.

(5) Hydrostatic pressure was decreased to the value for consolidation 1.

In Case 1, the specimen was unloaded and retrieved after compression 1 to observe fractures at the residual strength state.

Case 2 was to clarify the influences of consolidation 2. Case 2-1 was the base case in which hydrostatic pressure for consolidation 1, pore pressure and duration for consolidation 2 were set at 7 MPa, 5 MPa and 85 hours, respectively. In Case 2-2, duration for consolidation 2 was set at 24 hours. In Cases 2-3 and 2-7, the pressure for consolidation 2 was set at 50% residual strength. In Case 2-4, the confining pressure was set at 10 MPa.

In Case 3, (3)-(5) were repeated (compression 2 and consolidation 3).

In Case 4, the conditions for Case 2-1 were applied without compression 1.

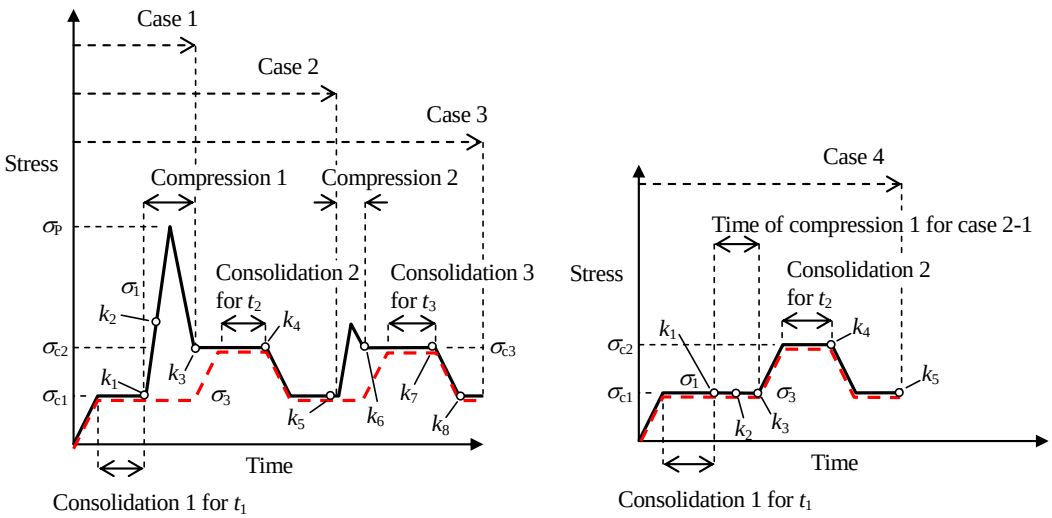

(a) Cases 1, 2-1, 2-2, 2-3, 2-4, 2-7 and 3 (b) Case 4

Fig. 1 Loading path. σ_1: axial stress, σ_3: confining pressure, σ_{c1}: consolidation stress 1 (initial consolidation), σ_{c2}: consolidation stress 2 (residual strength of compression 1 = $\sigma_1 = \sigma_3$), σ_{c3}: consolidation stress 3 (residual strength of compression 2 = $\sigma_1 = \sigma_3$), σ_p : peak stress, and k: permeability tests.

Table 1 Consolidation pressure and loading duration.

Rock	Case	σ_{c1} (MPa)	P_p (MPa)	t_2 (hr)	σ_{c2} (MPa)	σ_{c3} (MPa)
Kimachi sandstone	1	7	5	—	—	—
	2-1	7	5	85	19.2	—
	2-2	7	5	24	21.3	—
	2-3	7	5	85	11.6	—
	2-7	7	5	85	9.7	—
	2-4	10	5	85	32.6	—
	3	7	5	85	19.3	17.3
	4	7	5	85	19.2	—
Toyotomi siliceous mudstone		7	5	85	11.0	—
Inada granite		7	5	85	30.0	—

Permeability was measured based on the simplified transient pulse method by Brace et al. (1968). Confining pressure and axial stress were controlled to be constant during permeability measurements in the consolidations. On the other hand, confining pressure and circumferential strain were controlled to be constant during the permeability measurement in the axial loading to maintain the opening of axial microcracks constant during the measurement since the opening would most affect on permeability. The above controlling methods may have affected the measurement results. The latter

method however prevented sudden axial stress drops due to microcrack opening thereby enabling stable measurements.

The room temperature was controlled in the range between 297-299 K and the hydraulic conductivity was not corrected for that at 288 K. The following equations were used to evaluate hydraulic conductivity k (m/s).

$$\ln(P_1 - P_f) = \ln\left(\Delta P \cdot \frac{V_2}{V_1 + V_2}\right) - \alpha t \tag{1}$$

$$\alpha = \frac{kA}{\rho g \beta L} \cdot \frac{V_1 + V_2}{V_1 V_2} \tag{2}$$

where P_1 is the upstream pressure (Pa), V_1 and V_2 are the volume (m^3) of the upstream and downstream accumulator, respectively, P_f is the converged pressure (Pa), ΔP is the pressure pulse (Pa), t is the elapsed time (s), A is the sectional area (m^2), L is the specimen length (m), ρ is the water density (kg/m^3), g is the gravity acceleration (m/s^2) and β is the water compressibility (Pa^{-1}).

The post-failure hydraulic conductivity can be regarded as an equivalent one reflecting hydraulic conductivity of rock matrix and fractures. It however will be called just hydraulic conductivity for convenience in this paper. The hydraulic conductivity contains errors from the simplification in Brace et al. (1968) and usage of specimen sizes before any loading but the conductivity would be precise enough to be used to investigate change in permeability by post-failure consolidations.

Blue resin impregnated thin sections were prepared from specimens after experiments to observe the microstructure. The section was cut from the center of each specimen so that it became normal to the strike and parallel to the dip of the main rupture plane.

3. Results for Kimachi sandstone

3.1 Compression 1

Strains were set at zero under the atmospheric pressure. The residual strength was almost the same as the axial stress value at which the contracted diameter due to confining pressure recovered to zero by axial compression (Fig. 2). This phenomenon is not well known however Fujii et al. (1999) and Alam et al. (2014b) have already found for Inada granite and the mechanism was explained by the elastic block model in Fujii et al. (1999). The occasional stress relaxations (Fig. 2) were due to the above mentioned (in **2.3**) circumferential strain control during permeability measurement.

The rupture planes did not cross the specimen ends but reached the specimen side. A branched main rupture plane with small slip was observed for each specimen except for Case 2-3 in which a pair of conjugated rupture planes was observed.

Hydraulic conductivity before compression 1 (k_1) was in the range between 2.1-5.5 x 10^{-11} m/s except for 14.5 x 10^{-11} m/s for Case 3 (Table 2). Hydraulic conductivity began to decrease with compression 1 (Figs. 2-4) till the contraction of the specimen volume turned into dilatancy. Then the hydraulic conductivity began to increase up to the residual strength state (Fig. 3). The same behaviors have been observed by previous researches (Kiyama et al., 1997, Takada et al., 2011, Alam, et al., 2014a and b). The point at which the hydraulic conductivity began to increase also almost coincided to the point at which the circumferential contraction of the specimen recovered to zero by axial compression (Fig. 2). The minimum hydraulic conductivity k_2 was approx. 0.6-0.8 times that before the compression 1 (Table 2).

The hydraulic conductivity continued to increase in Cases 1, 2-4 and 3 but converged to a constant value in Cases 2-1, 2-2 and 2-3. The maximum hydraulic conductivity k_3 was 1.7-2.9 times of that before compression 1 (Table 2).

3.2 Consolidation 2 and unloading process for Cases 2 and 3

Axial and circumferential strains continued to show contraction during consolidation 2 (Fig. 4). The strains showed elongation due to unloading however did not recover to those values before consolidation 2 (Fig. 4) due to irrecoverable closure of fractures.

In Case 2-1, the hydraulic conductivity immediately decreased to 0.4 times k_1 by applying consolidation 2 (k_4) and slightly decreased during the consolidation. The hydraulic conductivity after unloading (k_5) was 0.7 times k_1 (Fig. 4, Table 2).

In Case 2-2 where duration of consolidation 2 was set at 30% that in Case 2-1, hydraulic conductivity after consolidation 2 (k_4) and after unloading (k_5) was 0.3 times and 0.6 times that before axial loading (k_1) (Table 2).

In Cases 2-3 and 2-7, hydraulic conductivity after unloading (k_5) was 0.4 and 0.6 times the maximum hydraulic conductivity (k_3) but 1.1 and 1.0 times that before axial loading (k_1). The reason of the higher k_5 would be the lower pressure at consolidation 2. Considering the k_5 value in Case 2-2 was the same as that in Case 2-1, the irrecoverable fracture closure did not strongly depend on the duration but strongly depended on the stress level in consolidation 2 within the conditions adopted in this study.

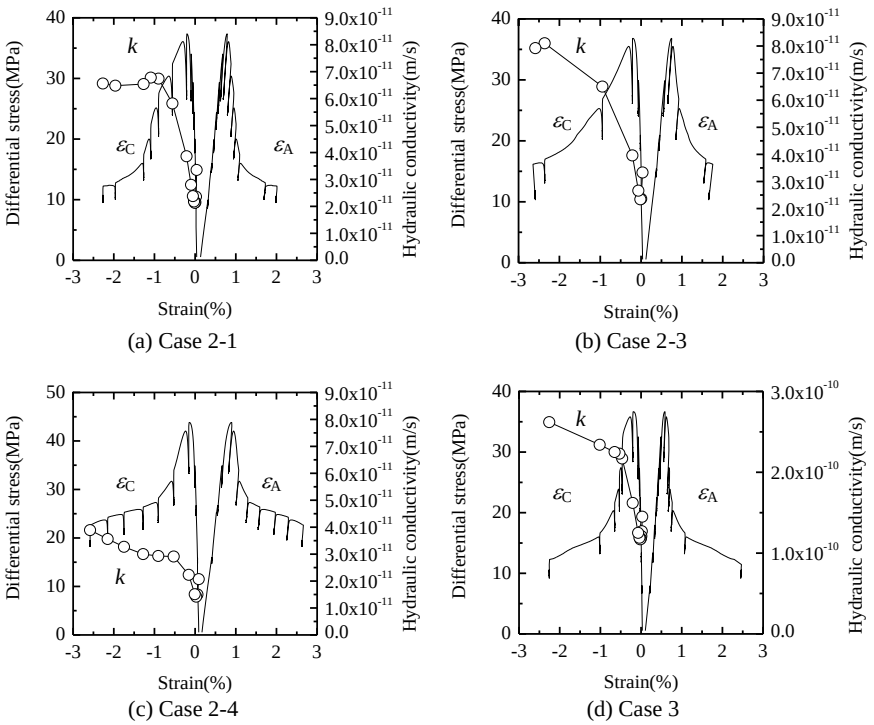

Fig. 2 Examples of stress-strain curves and hydraulic conductivity-circumferential strain curves for Kimachi sandstone. ε_A, ε_C, and k denote axial strain, circumferential strain and hydraulic conductivity. Strains were set at zero under atmospheric pressure.

Table 2 Hydraulic conductivities (k_1: end of consolidation 1, k_2: minimum value in compression 1 or consolidation 1 only for Case4, k_3: maximum value in compression 1 or consolidation 1 only for Case 4, k_4: end of consolidation 2, k_5: after consolidation 2, k_6: maximum value in compression 2, k_7: minimum value in consolidation 3 and k_8: after consolidation 3).

Rock	Case	k_1 (10^{-11} m/s)	k_2/k_1	k_3/k_1	k_4/k_1	k_5/k_1	k_6/k_1	k_7/k_1	k_8/k_1
Kimachi sandstone	1	5.45	0.68	2.86	—	—	—	—	—
	2-1	3.35	0.64	2.02	0.36	0.72	—	—	—
	2-2	4.73	0.64	1.66	0.31	0.60	—	—	—
	2-3	3.33	0.70	2.43	0.78	1.08	—	—	—
	2-7	4.09	0.77	1.71	0.81	0.97	—	—	—
	2-4	2.07	0.69	1.88	0.34	0.62	—	—	—
	3	14.5	0.81	1.81	0.56	0.83	0.97	0.52	0.74
	4	4.13	0.96	1.00	0.42	0.67	—	—	—
Toyotomi siliceous mudstone		5.17	0.93	1.29	0.56	0.57	—	—	—
Inada granite		1.41	0.60	73.0	3.87	15.8		—	—

In Case 2-4 where the effective confining pressure was 5 MPa while it was 2 MPa in other cases, hydraulic conductivity before compression 1 (k_1) was 0.4-0.6 times that for other cases. However k_2/k_1, k_3/k_1 and k_4/k_1 were almost the same as Cases 2-1, 2-2 and 2-3. This suggests that the difference between the confining pressure values was small and did not significantly affect in particular the post-failure permeability.

In Case 3, the extra compression and consolidation were carried out. Hydraulic conductivity after compression 2 (k_6) was almost the same as that before the axial loading 1 (k_1). Hydraulic conductivity values during the consolidations (k_4 and k_7) or after unloading (k_5 and k_8) were also almost the same (Table 2). This implies that the permeability of the post-failure rock does not significantly increase due to shear slip by further axial compression and does not contradict to the observation in triaxial compression tests for Kimachi sandstone up to 10% axial strain by Takada et al. (2011) and Alam et al. (2014a and b) in which permeability of rocks converged or slightly decreased in the residual strength state.

3.3 Consolidation 2 and unloading process for Case 4 (no axial loading)

In Case 4 where the specimen was not axially compressed to fail, the hydraulic conductivity decreased by consolidation 2 to 0.4 times and increased by unloading to 0.7 times that before compression 1 (Table 2). The ratios are almost the same as those in other cases and mean no significant influences of failure (Table 2). Similar results were obtained for Horonobe siliceous mudstone (Uehara et al., 2011 and Xue, 1992). The above findings may suggest that fractures do not significantly affect permeability of some clastic rock masses at certain depths.

3.4 Thin section observation

In Case 1 where consolidation 2 was not carried out, a basically straight and clear rupture plane was observed although there were some rock fragments surrounded by fractures just as islands (Fig. 5a). In Cases 2 and 3, the rupture planes were not continuous (Figs. 5b and 5c) due to fracture closure by consolidation 2 thereby causing the decrease in permeability. The observed unclear mesh like-fractures (Fig. 5b) may be new water paths formed around closed fractures. Fujii et al. (2011) has found similar networks of unclear fractures for Kushiro sandstone sampled at Kushiro Coal Mine, Japan. Similar capillary networks can also be observed around artery blockages in human bodies.

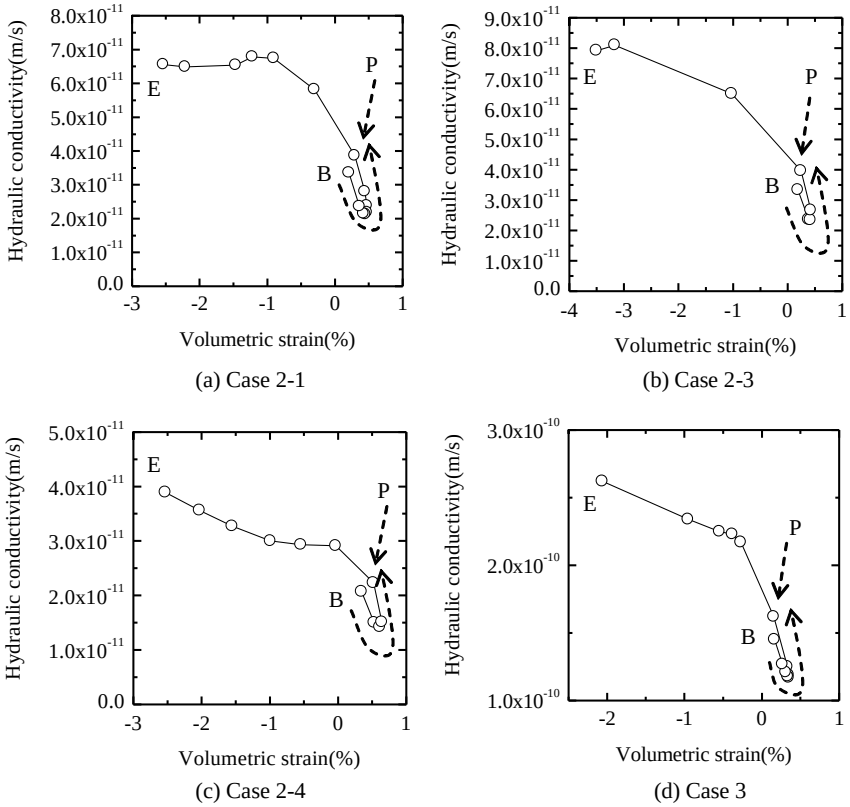

Fig. 3 Volumetric strain and hydraulic conductivity in compression 1 for Kimachi sandstone. B, E and P denote the beginning and the end of compression 1 and peak load point, respectively. The arrows denote the progress of tests.

4. Results for Toyotomi siliceous mudstone

Hydraulic conductivity decreased during compression 1 when the specimen volume was contracting and showed the minimum value around the peak load point (Fig. 6a). It then began to increase with the dilatancy and showed maximum value at the residual strength state (Figs. 6a-c). This behavior is similar to that for Kimachi sandstone. The stress level of the turning point from the decrease into increase was however around the peak load point for the rock while it was around 50% strength for Kimachi sandstone. The turning point did not coincide to the point where the circumferential strain recovered to its value due to axial compression. The hydraulic conductivity decreased by consolidation 2 to 0.56 times that before the compression 1 and slightly increased by unloading to 0.57 times (Fig. 6c and Table 2).

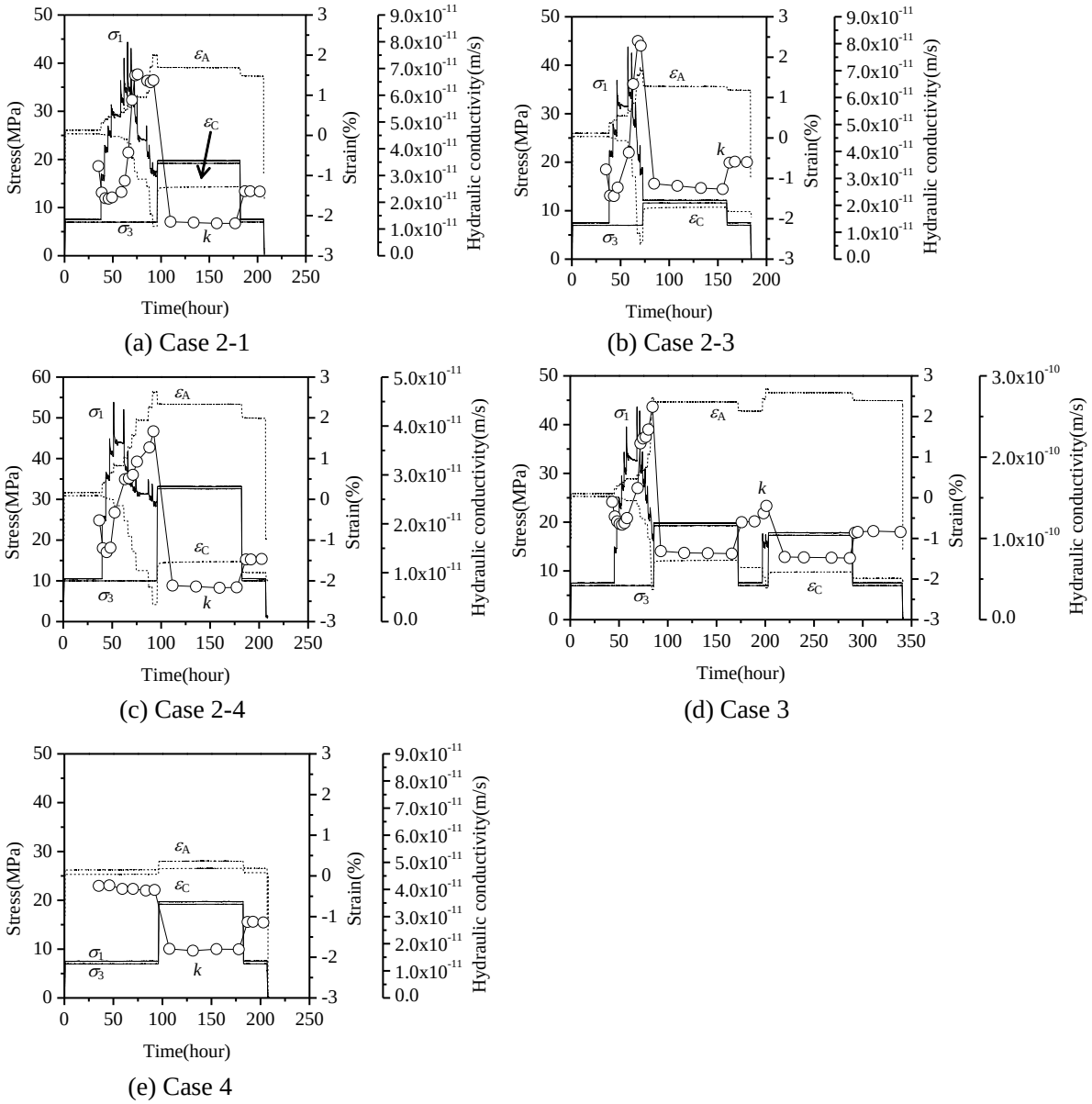

Fig. 4 Variation in strains and hydraulic conductivity during loading of Kimachi sandstone.

5. Results for Inada granite

Hydraulic conductivity decreased by compression 1 and then began to increase with dilatancy as other rocks (Fig. 7b). The turning point of the decrease into increase almost coincided with the point at which the contracted circumferential strain recovered to its value due to axial compression (Fig. 7c). The hydraulic conductivity increased to 73 times that before axial loading (Figs. 7a-c). The increase ratio was much more than 1.7-2.9 times for Kimachi sandstone and 1.3 times for Toyotomi siliceous

mudstone. The hydraulic conductivity immediately decreased by consolidation 2 and showed slight decrease during the consolidation to 3.9 times that before axial loading or 0.05 times the maximum value and then increased to 16 times that before axial loading or 0.22 times the maximum value by unloading.

6. Discussions

6.1 Change in hydraulic conductivity during compression 1

The hydraulic conductivity decreased until dilatancy began and then increased for all three rocks. The point where hydraulic conductivity turned from decrease into increase coincided to the point where the contracted circumferential length recovered to its value before loading for Kimachi sandstone and Inada granite. Toyotomi siliceous mudstone might have showed the different behavior due to the swelling during consolidation 1. The decrease in hydraulic conductivity at the initial stage of compression 1 was due to elastic and plastic closure of elliptic pores and microcracks which was not parallel to the loading axis and the succeeding increase was due to nucleation, growth and coalescence of microcracks.

6.2 Mechanisms of change in hydraulic conductivity due to post-failure consolidation

For Kimachi sandstone, such sand particles as quartz, feldspar, volcanic rock fragments are cemented mainly by clinoptilolite. Zeolites were weathered to such clay minerals as ion-rich saponite, montmorillonite etc. (Matsuki et al., 1998). The decrease in hydraulic conductivity was caused by closure of rupture plane due to crushing of mineral particles and plastic deformation of clay minerals composing rock matrix based on the results of strain measurements and thin section observations. The hydraulic conductivity increased by unloading but did not increase to the value before the axial compression since microcracks and elliptic pores in the intact rock matrix also irrecoverably closed by the post-failure consolidations.

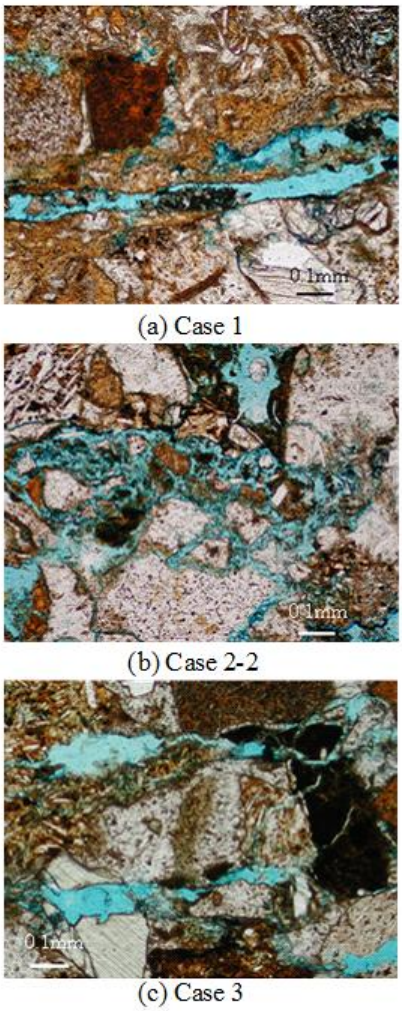

Fig. 5 Examples of thin section micrographs of Kimachi sandstone. Rupture plane is aligned parallel to horizontal.

Toyotomi siliceous mudstone clearly exhibited the time-dependent decrease in hydraulic conductivity during consolidation 2. Yasuhara et al. (2009) measured permeability of a granite specimen, which was sampled in Mizunami, Japan and had a discontinuity, under a confining pressure of 10 MPa at 293 K and 363 K for 550 hours. They explained the mechanisms of the permeability decrease mainly by pressure solution (ex. Green, 1984). It however is unlikely that pressure solution dominated considering the stress level and temperature of the present study. Rather, it is considered that a time-dependent closure of rupture plane due to visco-plastic deformation took place. A visco-plastic pore collapse also took place in the rock matrix since the hydraulic conductivity did not fully recover by the unloading. A possibility that some adhesion by mineral-water interaction may have occurred on parts of the rupture plane should be further investigated in future.

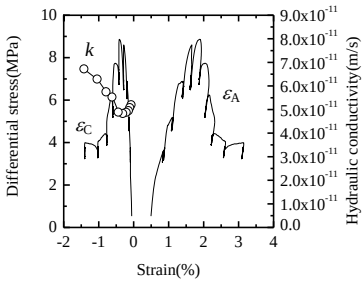

(a) Stress-strain curves and hydraulic conductivity-circumferential strain curve.

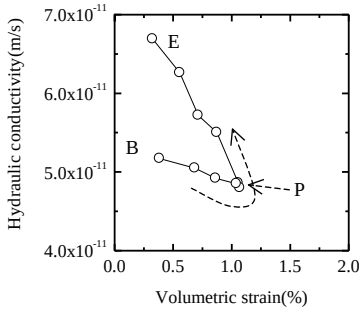

(b) Hydraulic conductivity-volumetric strain curve.

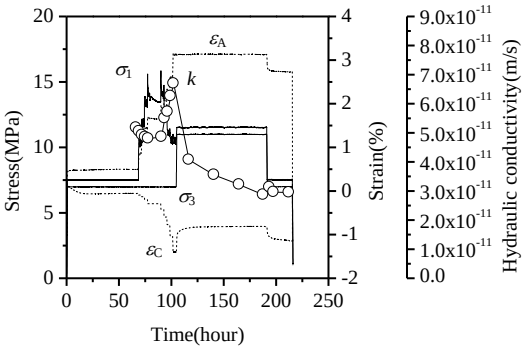

(c) Variation in strains and hydraulic conductivity due to loading.

Fig. 6 Results for Toyotomi siliceous mudstone.

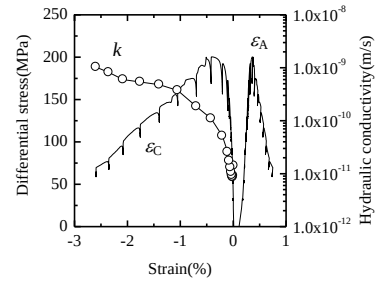

(a) Stress-strain curves and hydraulic conductivity-circumferential strain curve.

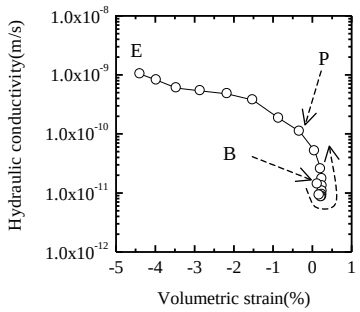

(b) Hydraulic conductivity-volumetric strain curve.

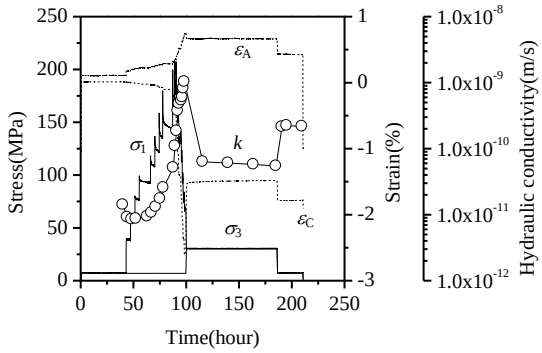

(c) Variation in strains and hydraulic conductivity due to loading.

Fig. 7 Results for Inada granite.

Post-failure hydraulic conductivity of Inada granite was 73 times that before axial compression 1. This is because the aperture of the rupture plane was large since the plane was rough and did not consist of soft rock matrix but consisted of hard mineral particles. The decrease of hydraulic conductivity during consolidation was still high because the rock was stiff and the consolidation stress was relatively small compared to the rock strength thereby inducing a small elastic deformation. A little visco-plastic deformation and a few pressure solution at stress concentration points on the rupture plane can be mechanisms of the time-dependent slight decrease of hydraulic conductivity during the consolidation. There should be neither a large visco-plastic deformation of microcracks in intact rock nor obvious adhesion or large irrecoverable closure by pressure solution since the hydraulic conductivity increased to 4 times by unloading.

7. Concluding remarks

Post-failure consolidation was carried out on Kimachi sandstone, Toyotomi siliceous mudstone and Inada granite to clarify whether the increased hydraulic conductivity due to failure decreased by post-failure consolidation or not. The hydraulic conductivity of post-failure consolidated rocks were 0.3-0.6 times that before post-failure consolidation and 0.9-1.5 times that before failure for Kimachi sandstone and the ratios were 0.4 times and 0.6 times for Toyotomi siliceous mudstone. On the other hand, the ratio was 0.2 times and 16 times for Inada granite. Namely, the phenomenon in which the increased hydraulic conductivity decreases by post-failure consolidation was obviously confirmed for the clastic rocks and was confirmed at some degree for the crystalline rock. It is hoped to accumulate data by similar or sophisticated experiments and to utilize them for reasonable designing of underground repositories in future.

The dominating mechanisms of decrease in hydraulic conductivity due to the post-failure consolidations were considered to be closure of rupture plane by crushing of mineral particles and irrecoverable closure of microcracks and elliptic pores in intact rock matrix due to plastic deformation for Kimachi sandstone, time-dependent closure of rupture plane due to visco-plastic deformation and visco-plastic pore collapse in intact rock matrix for Toyotomi siliceous mudstone, and a little visco-plastic deformation and a few pressure solution at the rupture plane for Inada granite. The different mechanisms were mainly induced by the differences in strength and deformation characteristics of mineral particles and rock matrixes. Further investigations are of course required since the above considerations are not strongly supported yet by precise analyses.

References

Alam, B., Fujii, Y., Fukuda, D. and Kodama, J., 2014a, submitted, Fractured rock permeability versus rising temperature and pressure: relevance to burial of radioactive waste, *Int. J. Rock Mech. Min. Sci.*

Alam, B., Niioka, M., Fujii, Y., Fukuda, D and Kodama, J., 2014b, Effects of confining pressure on the permeability of three rock types undercCompression, *Int. J. Rock Mech. Min. Sci.*, 65, 49-61.

Brace, W. F., Walsh, J. B. and Frangos, W. T.,1968, Permeability of granite under high pressure, *J. Geophys. Res.*, 73, 2225-2236.

Buehler, Ch., Heitz, D., Trick, Th., Frieg, B., 2003, In situ self-sealing of the EDZ as a consequence of loading, *Proc. EC CLUSTER Conference and Workshop Luxembourg, 3 to 5 Nov. 2003*, 281-286.

Fujii, Y., Ishijima, Y., Ichihara, Y., Kiyama, T., Kumakura, S., Takada, M., Sugawara, T., Narita, T., Kodama, J., Sawada, M. and Nakata, E., 2011, Mechanical properties of abandoned and closed roadways in the Kushiro Coal Mine, Japan, *Int. J. Rock Mech. Min. Sci.*, 48, 585-596.

Fujii, Y., Ishijima, Y. and Kiyama, T., 1999, Confining pressure-dependency of coefficients in the simple constitutive equations for brittle rock, *Proc. '99 Japan-Korea Joint Symp. on Rock Engineering*, 323-330.

Green II, H. W., 1984, "Pressure solution" creep: some cause and mechanisms, *J. Geophys. Res.*, 89, 4313-4318

Kiyama, T., Sato, T., Cho, A., Yanagitani, S. and Ishijima, Y., 1997 in Japanese, Influences of damage on permeability of rock, *Proc. MMIJ Fall Meeting*, 65-68.

Matsuki, K., Sakaguchi, K., Iino, H., Okumura, K., 1998 in Japanese, Effects of pore pressure on strength of sedimentary rocks, J. MMIJ, 114, 895-900

Ohishi, Y., Hashiba, K. and Fukui, K., 2014 in Japanese, Impermeability Recovery of Fracture Rocks, *Proc. MMIJ Spring Meeting*, 14-3.

Takada, M., Fujii, Y. and Kodama, J., 2011 in Japanese, A study on influences of confining pressure on permeability of rock, *J. MMIJ*, 127, 151-157.

Tsang, C.−F., Bernier, F. and Davies, C., 2005, Geohydromechanical processes in the excavation damaged zone in crystalline rock, rock salt, and indurated and plastic clays−in the context of radioactive waste disposal, *Int. J. Rock Mech. Min. Sci.*, 42, 109−125.

Uehara, S., Shimaoto, T., Matsumoto, T., Sinsato, T., Okazaki, K. and Takahashi, Y., 2011 in Japanese, Fracture permeability of Neogene muddy soft rocks, *J. MMIJ*, 127, 139-144.

Xue, Z. (1992 in Japanese), An experimental study on relationship between permeability and microstructure of sandstone, *Dissertation for Graduate School of Engineering, Hokkaido University*.

Yasuhara, H., Kinoshita, N., Lee, D. S., Nakajima, S. and Kichida, K., 2009 in Japanese, Predictions of hydraulic and transport behavior in a agrante fracture via coupled mechano-chemo conceptual model, *Doboku Gakkai Ronbunshuu C*, 65, 41-52